



The greening of the Northern Great Plains and its biogeochemical precursors

*E.N.J. Brookshire¹,

Paul C. Stoy^{1,2},

Bryce Currey¹,

Bruce Finney³

¹ Department of Land Resources and Environmental Sciences, Montana State University

² Department of Biological Systems Engineering, University of Wisconsin – Madison

³ Departments of Biological Sciences and Geosciences, Idaho State University

*406-994-3973; jbrookshire@montana.edu

Vegetative greening, water use efficiency, nitrogen cycle, nitrogen use efficiency, isotopes, climate, Northern Great Plains, grasslands

This article has been accepted for publication and undergone full peer review but has not been through the copyediting, typesetting, pagination and proofreading process, which may lead to differences between this version and the [Version of Record](#). Please cite this article as [doi: 10.1111/gcb.15115](https://doi.org/10.1111/gcb.15115)

This article is protected by copyright. All rights reserved

Abstract

Vegetation greenness has increased across much of the global land surface over recent decades. This trend is projected to continue – particularly in northern latitudes – but future greening may be constrained by nutrient availability needed for plant carbon (C) assimilation in response to CO₂ enrichment (eCO₂). eCO₂ impacts foliar chemistry and function, yet the relative strengths of these effects *versus* climate in driving patterns of vegetative greening remain uncertain. Here, we combine satellite measurements of greening with a 135-year record of plant C and nitrogen (N) concentrations and stable isotope ratios ($\delta^{13}\text{C}$ and $\delta^{15}\text{N}$) in the Northern Great Plains (NGP) of North America to examine N constraints on greening. We document significant greening over the past two decades with the highest proportional increases in net greening occurring in the driest and warmest areas. In contrast to the climate-dependency of greening, we find spatially uniform increases in leaf-level intercellular CO₂ (C_i) and intrinsic water use efficiency (iWUE) that track rising atmospheric CO₂ (C_a). Despite large spatial variation in greening, we find sustained and climate-independent declines in foliar N over the last century. Parallel declines in foliar $\delta^{15}\text{N}$ and increases in C:N ratios point to diminished N availability as the likely cause. The simultaneous increase in greening and decline in foliar N across our study area points to increased N use efficiency (NUE) over the last two decades. However, our results suggest that plant NUE responses are likely insufficient to sustain observed greening trends in NGP grasslands in the future.

1 | INTRODUCTION

Field experiments and ecosystem models suggest that recent vegetative greening is largely explained by CO₂ enrichment (eCO₂), climate change, N deposition, and land cover change (Huang et al., 2018; Zhu et al., 2016). While the relative importance of these drivers varies geographically (Huang et al., 2018; Mao et al., 2016; Myneni et al., 1997; Zhu et al., 2016), eCO₂ is the most spatially uniform and its direct effects on plant physiology are well understood. Free-atmosphere CO₂ enrichment (FACE) studies show increased plant carbon (C) assimilation and photosynthetic nitrogen (N) use efficiency (NUE) with eCO₂ (Feng et al., 2015; Leakey et al., 2009; Terrer et al., 2018). These effects are strongest among C₃ plants that dominate land-atmosphere C exchange globally (Still et al., 2003). However, these studies also show that foliar N concentrations decline by ~6 - 12% below that at

ambient CO₂ due to diminished N acquisition (Feng et al., 2015), availability (Reich & Hobbie, 2013), or assimilation (Busch et al., 2017).

Nitrogen is fundamental to C assimilation and protein synthesis in leaves and thus could constrain greening, particularly in N-limited ecosystems. Herbarium and tree-ring analyses indicate that declines in plant N have already occurred across some temperate biomes over the last century despite increases in N deposition (Craine et al., 2018; McLauchlan et al., 2017; McLauchlan et al., 2010; Peñuelas & Estiarte, 1996; Peñuelas & Matamala, 1990), consistent with the hypothesis that N is constraining greening (Hungate et al., 2003; Luo et al., 2004; McMurtrie et al., 2008). Simultaneously, these studies document large and persistent increases in plant iWUE in response to eCO₂ (Frank et al., 2015; McLauchlan et al., 2010), a response that reduces water costs per unit C assimilated and thus could potentially sustain vegetative greening, particularly in drier regions (Zhu et al., 2016).

It is unclear whether increased iWUE and/or NUE can compensate for increasing N demand under scenarios of enhanced vegetative productivity. Insight into these processes can be gained by understanding how leaf-level intercellular CO₂ (C_i) the core substrate for photosynthesis, has changed relative to atmospheric CO₂ (C_a) over time. Nitrogen and C_i are fundamentally coupled through the action of the Rubisco enzyme, which typically accounts for ~25% of leaf N (Leakey et al., 2009). If C_i/C_a ratios remain roughly constant, eCO₂ would drive increases in C_i and photosynthetic C assimilation. Given the strong dependence of C assimilation on C_i , alternative explanations that result in constant C_i imply large reductions in stomatal conductance (Guerrieri et al., 2019) and potentially constant leaf N/ C_i ratios depending on physiological responses to increasing C_a . Under N-limited conditions, however, FACE results document Rubisco acclimation, declines in Rubisco content, accumulation of foliar carbohydrates (Leakey et al., 2009) and declines in photorespiratory N assimilation (Busch et al., 2017) under eCO₂. Knowledge of C_i change is crucial for understanding changes in plant NUE and C:N stoichiometry, which can drive ecosystem-level N availability via effects on microbial N immobilization and mineralization (Luo et al., 2004). However, the role of these key interactions in shaping recent and future vegetation changes remain poorly understood.

Temporal changes in the $\delta^{15}\text{N}$ composition of leaves offers one way to diagnose long-term change in the plant-soil N cycle. While several processes can imprint on $\delta^{15}\text{N}$ in foliage including

external N inputs, mycorrhizal discrimination, and enzymatic discrimination during nitrate assimilation, numerous lines of evidence also indicate that the leaf $\delta^{15}\text{N}$ signature tracks changes in inorganic N availability (Craine et al., 2009), consistent with increasing microbial fractionation in soils as inorganic N availability increases (Craine et al., 2015). Declines in foliar $\delta^{15}\text{N}$ in response to experimental $e\text{CO}_2$ have been documented across numerous plant types and ecosystems (BassiriRad et al., 2003) and long-term declines in $\delta^{15}\text{N}$ from herbarium and tree-ring studies have been documented over the last century across many ecosystems globally (Craine et al., 2018; McLauchlan et al., 2017; McLauchlan et al., 2010; Peñuelas & Estiarte, 1996), suggesting direct or indirect effects of $e\text{CO}_2$ on N availability. Yet, it is unclear how the recent increases in vegetative productivity, which in the northern hemisphere has been evident since at least the 1960's (Keeling et al., 1996), relate to changes in plant N and $\delta^{15}\text{N}$ in N-limited ecosystems and if these relationships vary across climatic gradients.

The extent to which changes in foliar chemistry and vegetative activity are coupled in space and time may provide insight into the relative strength of global change drivers. For example, while the rise in C_a has directly increased plant $i\text{WUE}$ through enhanced photosynthesis in addition to reduced transpiration through stomata (Guerrieri et al., 2019), much of the recent increase in northern hemisphere vegetative greening is thought to be driven by changes in climate and increased growing season length. For N, the degree to which changes in plant N may also be coupled directly or indirectly to $e\text{CO}_2$ and greening is less clear.

Here, we combine satellite observations of recent vegetation greening trends with chemical and isotopic analyses of historical plant samples to examine responses of vegetative productivity to $e\text{CO}_2$ and climate in the Northern Great Plains (NGP) of North America. The NGP is one of the largest relatively intact temperate grasslands worldwide (Auch et al., 2011), is strongly N-limited (Burke et al., 1997), has experienced a strong wetting trend over the last twenty years (Bromley et al., 2019; Rodell et al., 2018) and is projected to experience increases in growing season precipitation (Stoy et al., 2018) and vegetation greening (Hufkens et al., 2016; Reeves et al., 2014; Shafer et al., 2015) over the next century. To examine the spatial and temporal correspondence of any potential changes in foliar chemistry and vegetative greening, we analyzed monthly Moderate Resolution Imaging Spectroradiometer (MODIS) normalized difference vegetation index (NDVI) data as a proxy

for photosynthetically active vegetation across the NGP for the 2000-2018 period and leaf C and N concentrations and stable isotopes of common C3 plants collected from 1881 to 2016 across 390 grassland sites spanning broad environmental gradients across the NGP and Northern Rocky Mountain (NRM) ecoregions (Supplementary Table 1) in the U.S. State of Montana (MT; Fig 1a,b). As mean climate is on average considerably cooler and wetter in the NRM compared to the NGP, we used this contrast to evaluate the climate sensitivity of any changes in vegetative activity and foliar iWUE, chemistry and $\delta^{15}\text{N}$ and their interactions.

2 | MATERIALS AND METHODS

2.1 | Satellite NDVI data

NDVI data were derived from the NASA's MODIS Vegetation Indices 16-day L3 Global product (MOD13A1, Version 6) at a 0.5 km spatial scale. Pixel-level NDVI is generated from daily surface-reflectance data aggregated every 8-days and composited every 16-days, from which the maximum value is selected at each pixel. An annual time series of bi-monthly NDVI values were used to calculate annual maximum NDVI. We used a two-sided Mann-Kendall trend test to determine which pixels showed significant ($p < 0.05$) positive or negative change over the 2000 - 2018 period. For pixels showing positive ("greening") or negative ("browning") NDVI change overtime, we calculated percent change relative to the initial NDVI value. In total, we analyzed changes in NDVI across 1,037,074 pixels comprising the entire NGP and 616,199 pixels spanning the NGP and NRM of MT. For each region, we determined net greening rates by multiplying the fraction of pixels showing significant positive, negative, or no NDVI change by their respective mean (\pm geometric SD) magnitude NDVI change (% yr⁻¹).

2.2 | Climate and nitrogen deposition

We estimated mean annual temperature (MAT) and precipitation (MAP) across the NGP and NRM of MT using CHELSA (Climatologies at high resolution for the earth's land surface areas) data of downscaled model output temperature and precipitation at 1 km resolution for the 1980-2018 period (Karger et al., 2017). We also used PRISM (Parameter-elevation Regressions on Independent Slopes Model; <http://prism.oregonstate.edu>) to calculate the long-term (1890- 2016) growing season (May-

August) Palmer Drought Severity Index (higher values indicate wet conditions and lower values indicate drought) for major hydrologic units in the NGP (Fort Peck Reservoir, Big Horn, Powder River) and NRM (Marias, Missouri Headwaters, Upper Yellowstone) of MT in which most of our plant samples were collected and for the individual coordinates of our field collections. To examine long-term patterns of external N inputs, we used annual bulk $\text{NO}_3\text{-N} + \text{NH}_4\text{-N}$ deposition measured from 1984 to 2017 by the National Atmospheric Deposition Program at five stations in MT (MT00, MT07, MT98, MT96, MT97).

2.3 | Herbarium data

We selected four native C3 grassland species (*Artemisia tridentata*, *Festuca idahoensis*, *Koeleria macrantha*, *Pseudoregenaria spicata*; Table S1) for study based on 1) documented broad geographic distribution and high relative abundance across NGP and NRM grasslands (Lavin & Seibert, 2011; Mueggler et al., 1980) and 2) broad spatial representation of herbarium type specimens in the Consortium of Pacific Northwest Herbaria (CNHP) database (<http://www.pnwherbaria.org>) for which Montana samples are housed at the Montana State University Herbarium. Though C4 grass species occur within our study area, these species compose a small proportion of Montana grassland communities. The CNHP records the spatial coordinates, date of sampling and site descriptions documented by the original botanical collectors. We accessed all available specimens of our study species and sampled small sections of leaf material from 3-5 leaves per specimen based on availability. Sub-samples of each specimen were gently cleaned with a brush and were composited and ground for chemical and isotopic analysis.

2.4 | Plant resampling

In 2016, we resampled plants from a randomly chosen subset ($n = 80$) of the original site locations (Supplementary Table 1). We incorporated historical site descriptions to relocate the original sampling location given potential inaccuracies in the reported coordinates and altitude and resampled within three weeks of the original collection date. Sites with significant disturbance or land-use change or that were not publicly accessible were excluded. After field collections, we cross-checked our recorded site altitudes with those of historical samples and excluded those that differed by > 100

m to avoid potential effects of climate and atmospheric pressure on chemical and isotope distributions. Resultant samples ($n = 68$) were processed identically to the historical herbarium specimens.

2.5 | Chemical and isotopic analyses

Samples for carbon and nitrogen concentrations and stable isotope ratios were analyzed at the Idaho State University Stable Isotope Laboratory using a Costech ECS 4010 elemental analyzer interfaced with a Thermo Delta V Advantage continuous flow isotope ratio mass spectrometer. All stable isotopic data are reported in standard delta notation ($\delta^{13}\text{C}$, $\delta^{15}\text{N}$) relative to the Vienna PeeDee Belemnite (VPDB) and atmospheric N_2 reference standards. Analytical precision, calculated from analysis of standards distributed throughout each run, was $\leq \pm 0.2\text{‰}$ for both C and N stable isotopes, and $< \pm 0.5\%$ of the sample value for $\% \text{N}$ and $\% \text{C}$. To account for the changing ^{13}C signature of atmospheric CO_2 , we used the average $^{13}\text{CO}_2$ signature for June–September months spanning the 1978–2016 period recorded at La Jolla, CA and Point Barrow, AK, USA (Scripps Institution of Oceanography). To derive CO_2 and $^{13}\text{CO}_2$ signatures for the period 1881–1978, we used ice-core records (Francey et al., 1999) and interpolated missing data using a spline function. We calculated ^{13}C discrimination (Δ) as

$$\Delta = \frac{\delta^{13}\text{C}_{\text{air}} - \delta^{13}\text{C}_{\text{plant}}}{1 + \delta^{13}\text{C}_{\text{plant}}/1000} \quad (1)$$

which we used to derive C_i/C_a , C_i , and iWUE by applying isotope fractionation constants for carboxylation (b , 27‰) and diffusion (a , 4.4‰; Farquhar, Ehleringer, & Hubick, 1989).

$$\frac{C_i}{C_a} = \frac{\Delta - a}{b - a} \quad (2)$$

$$C_i = \frac{C_a \times \Delta - C_a \times a}{b - a} \quad (3)$$

$$iWUE = \frac{C_a \times \left(1 - \frac{C_i}{C_a}\right)}{1.6} \quad (4)$$

2.6 | Statistical analyses. We analyzed changes in regional climate and foliar chemistry and isotopes over time using a combination of linear and non-linear regression and breakpoint analysis to detect changes in slope using packages “nlme” and “segmented” in R. For break-point analyses, we used Z-scores of foliar chemistry and isotope data to visualize long-term dynamics on a common scale. We examined the relative strength of eCO₂ versus climate effects on foliar chemistry and δ¹⁵N using linear mixed effects models either with C_a or C_i as fixed effects and species, year, or climate as random effects or with climate as a fixed effect and species and year as random effects. We retained species as a random effect in all models. To examine climate in these models we used the growing season PDSI which has been shown to predict climate sensitivity in MT grasslands (Brookshire & Weaver, 2015). Because PDSI did not change directionally over time while C_a did, we nested species within year to isolate climate effects from non-linear increases in C_a due to eCO₂. We chose models with lowest corrected Akaike Information Criterion (AICc) using an AICc difference (ΔAICc) between models > 2 as a significance cutoff (Anderson, 2007); all models were best explained without climate effects. We developed species-specific C_i response curves using the general form

$$N_s = \frac{N_{min} \times C_i}{k_m + C_i} \quad (5)$$

where N_s is the species-specific response variable (i.e., %C, %N, δ¹⁵N), N_{min} is the minimum (or maximum) value and k_m is the half-saturation constant. While linear regressions generally explained foliar responses to C_i equally well as saturating functions (ΔAICc < 2), we assumed that C and N concentrations have species-specific physiological minima and maxima and thus cannot increase or decrease indefinitely or fall below zero, as linear regressions imply. Finally, to simulate potential maximum changes in foliar chemistry in response to future eCO₂ we applied RCP 8.5 projected atmospheric CO₂ for year 2100 to species specific CO₂-C_i regressions and functional curves for %C, %N, and molar C:N ratios.

3 | RESULTS

3.1 | Recent trends in vegetative activity

We document extensive vegetative greening across the NGP biome over the last two decades. Sustained increases in NDVI were evident across >19% of the land area at an average rate of 1.2% yr⁻¹, a 22% increase since 2000. By combining the distribution and rates of browning (declining NDVI) pixels, we calculate a net positive increase in peak vegetative activity greater than 0.2% yr⁻¹ across the NGP as a whole. Greening rates were especially pronounced across the MT portions of the NGP (Figure 1, Table 1). In contrast, net greening rates were four-fold lower in the mountainous and largely forested NRM part of our study area. This difference resulted from higher proportion of the NRM that experienced browning and a greater than two-fold lower magnitude of increase among greening pixels compared to the NGP.

Comparing long-term (1980-2018) mean climate across our MT study area with recent changes in NDVI revealed that greening trends were more prevalent in the driest and warmest areas and increased most strongly with increasing MAT (Figure 2a) and declining MAP (Figure 2b) in the NGP compared to the NRM. The spatial locations of our historical plant samples are well represented across the geographic distribution of vegetative trends and climate space within our study area (Figure 2c).

3.2 | Long-term changes in foliar chemistry and isotope distributions

Despite large variation in mean annual climate (Figure 2a,b) and decadal variation in growing season climate across our study area (Figure 3a), C_i increased in all species regardless of geographic location (Figure 3c), while isotopic discrimination and C_i/C_a ratios remained constant (Figure S1). The increase in C_i accelerated sharply in the 1970s (break-point analysis mean and standard deviation: 1973 ± 4 ; $p < 0.001$; Figure 3c) and was strongly correlated with C_a but not changes in climate (Figure S1). Accordingly, we find that iWUE has increased on average by 37% over the last century, most of which (85%) has likewise occurred since the early 1970's (1971 ± 4 ; $p < 0.001$; Figure 3e). Although the magnitude of response varied among species (27 - 53%), it did not vary systematically across climate regions.

The timing and spatial uniformity of increases in C_i and iWUE suggest a direct effect of eCO_2 on leaf-level physiology regardless of climate. We next assessed whether leaf C and N concentrations have responded in an analogous manner or have changed in response to changing climate or atmospheric N deposition. Foliar C concentrations increased significantly over time ($0.4 \pm 4 \text{ mg g}^{-1}\text{yr}^{-1}$, $p < 0.001$) but did not show a clear breakpoint nor vary as a function of PDSI. In contrast, foliar N concentrations declined significantly ($p < 0.01$) across all study species, but the decline began in the 1930's (1931 ± 13 years), roughly four decades prior to steep increases in C_a and iWUE and has not recovered since (Figure 3d). Foliar $\delta^{15}\text{N}$ also decreased by $\sim 10\%$ uniformly across the NGP and the NRM beginning in the late 1930's (1937 ± 13 years; $p < 0.01$; Figure 3f). While we found no long-term relationship between either foliar N and PDSI or $\delta^{15}\text{N}$ and PDSI ($p > 0.1$ in mixed effects models using species and year as random effects; Figure S2), we document that the onset of declining foliar N and $\delta^{15}\text{N}$ corresponded closely with the "Dust Bowl" drought of the 1930's (Figure 3a, d, f). In contrast to sustained declines in foliar N, measured N deposition rates have more than doubled ($0.028 \text{ kg N ha}^{-1} \text{ yr}^{-1}$) since the 1980's (Figure 3b), but have remained relatively low (long-term deposition rate of $1.1 \pm 0.6 \text{ kg N ha}^{-1} \text{ yr}^{-1}$) over the recent period of vegetative greening in the NGP.

We next asked if these findings, which rely on statistical fitting across samples collected at different years and locations, persist after controlling for geographic location. Analysis of our spatially-paired samples confirms the magnitude and direction of change observed in the full data set. On average, foliar C concentrations increased by $10 \pm 1\%$ (4 - 17% among species), N decreased by $12 \pm 3\%$ (6 - 18%), C:N ratios increased by $19 \pm 3\%$ (13 - 30%) and $\delta^{15}\text{N}$ decreased by $10 \pm 2\%$ (6 - 18%) independent of wide variation in local growing season climate (Figures S3, S4). Further, there was no evidence ($p > 0.05$) within and across species that proportional declines in leaf N or $\delta^{15}\text{N}$ depend on increases in C, as would be expected if declines were driven by foliar mass dilution.

Finally, we examined how foliar chemistry and $\delta^{15}\text{N}$ may have changed in response to non-linear increases in leaf C_i . We focused our analysis on the reduced (spatially paired) data set to control for local differences in climate and soil resource availability. Foliar C and C:N increased and N and $\delta^{15}\text{N}$ decreased significantly ($p < 0.01$) in response to the > 100 ppm increase in C_i over the last century (Figures 4a-d). Further, across broad geographic areas and climate zones, our four study species converged toward an increasingly similar and narrow range of foliar chemistry with

increasing C_i . Relatively C-rich species tended to show small increases in C concentrations while C-poor species showed steep increases in C concentrations. Likewise, the decline in foliar N was largest for species with initially high N concentrations and relatively small for initially low-N species. Despite asymptotic increases in foliar C (Figure 4a), steeper increases in C_i (Figure 3c) translate to average declines in both internal leaf C/C_i ratios of $-17 \pm 4\%$ with the historical rise in eCO_2 , suggesting progressively diminishing returns on C accumulation per unit CO_2 uptake. Similarly, declines in foliar N (Figure 4b) translate to an average N/C_i decline of $-30 \pm 8\%$. By applying these functional C_i relationships to projected aCO_2 of 935.8 ppm for year 2100 we estimate that average foliar C_i would be 641.2 ± 40.6 ppm, foliar C would rise by 10% (from 457 ± 21 mg g^{-1} to 505 ± 26 mg g^{-1}), N would decline by 12% (from 13.2 ± 0.2 mg g^{-1} to 11.6 ± 0.1 mg g^{-1}) and C:N ratios would increase by 18% (from 42.9 ± 5.9 to 50.5 ± 2.6) relative to 2016.

4 | DISCUSSION

We document extensive vegetative greening of North America's northern grassland biome over the last two decades. This trend is consistent with widespread and large increases in plant foliar C_i and $iWUE$ that correspond to the rise in eCO_2 since the 1970's. While net vegetative greening rates were most pronounced in the driest and warmest areas of our study region, the direction and magnitude of long-term changes in foliar C_i , $iWUE$, C, N, and $\delta^{15}N$ did not vary across climates. The spatial uniformity of changes in foliar chemistry across the broad climate gradients sampled contrast with the climate-dependency of recent greening and suggests that any realized gains in vegetative growth due to direct effects of eCO_2 at the leaf level were modulated by climate. We find that grassland vegetation across our diverse study area has become increasingly water conservative, C rich, and N poor over the last century.

Across the NGP, NDVI increased on average $0.28\% \text{ yr}^{-1}$, a value similar to model projections for the broader NGP spatial domain over the next century (0.19 - 0.45% yr^{-1} ; Hufkens et al., 2016; Reeves et al., 2014). Our finding of higher net greening rates in the NGP than in the NRM is consistent with larger increases in growing season precipitation and decreasing vapor pressure deficit in the NGP than the NRM since the mid-1980's (Bromley et al., 2019; Gerken et al., 2017) but is also likely influenced by the smaller areal distribution of grassland vegetation in the NRM. Overall, annual

net primary production is substantially higher in the NRM compared to the grassland-dominated NGP. However, forest vegetation across much of the NRM has been subject to wildfire and insect-outbreak mortality over the last few decades (Emmett et al., 2018) while the NGP has not, consistent with the lower per-pixel positive greening rate and spatially more extensive vegetative browning rate. While our foliar analyses focused entirely on grassland plant species, our analysis of peak NDVI changes did not distinguish between grassland and forest vegetation. Despite these differences, our finding of increasing iWUE among common plant species distributed across broad climate gradients suggests a direct effect of eCO₂, an inference supported by the timing of sharp increases in iWUE beginning in the 1970s which preceded regional increases in precipitation and water availability (Bromley et al., 2019; Rodell et al., 2018) by decades.

Constant C_i/C_a ratios across modern climates suggests that plants have uniformly adjusted stomatal regulation in response to eCO₂. Our findings of constant and climate-independent increases in iWUE with rising CO₂ are consistent with optimal stomatal regulation theory (Farquhar et al. 1980), FACE observations (Medlyn et al., 2011) and vegetation paleo-isotope results from other regions (Frank et al., 2015), and provide support for the generality of a strong direct effect of eCO₂ on foliar water-CO₂ exchange. That the NGP has experienced significant increases in vegetative productivity over the last few decades is also consistent with a direct contribution of enhanced photosynthesis to increased iWUE (Guerrieri et al., 2019)

The difference in the timing of historical changes in foliar C_i versus N concentrations offers insight into the degree to which these changes were physiologically coordinated in response to eCO₂ or were independent responses to different forcings. We document a sustained decline in plant N and $\delta^{15}\text{N}$ that preceded the rise in eCO₂ and recent greening by over a half century. While CO₂ levels during the 1930s were elevated relative to pre-industrial concentrations (~5%), the growth in eCO₂ didn't accelerate until the 1960's. Nevertheless, given that N availability in the NGP is low (Burke et al., 1997), it is possible that marginal increases in CO₂ prior to the 1930's increased N demand sufficiently to lower soil N, although such declines in foliar N have been experimentally observed to occur only after doubling of CO₂ (Leakey et al., 2009). Another possibility is that changes in N inputs contributed to the decline in foliar N and $\delta^{15}\text{N}$. However, N deposition to our study region is low, and while N deposition has increased by greater than two fold over the last couple decades (from ~0.6 to

~1.6 kg N ha⁻¹ yr⁻¹) this represents only ~3-7% of N mineralization (i.e., internal N supply to plants) across the NGP (Burke et al., 1997). While we do not have measures of the isotopic signature of N deposition across our study area, nor how it has changed over time, attribution of the isotopic shift to atmospheric deposition would imply substantial reliance on this source for plant assimilation and would require an isotopic signature lower than generally recorded (Houlton & Bai, 2009). Moreover, any increase in N supply should yield increases in foliar N, not decreases as we observe.

Our break point analysis suggests an alternative explanation for the onset of N and $\delta^{15}\text{N}$ declines that may have resulted from a climatic and/or land-use perturbation. The documented declines in N and $\delta^{15}\text{N}$ in the 1930's show a tight temporal correspondence to an historically unprecedented drought during the Dust Bowl (Fye et al., 2003). Though we lack information on potential mechanisms involved (e.g., soil erosion, loss of microbial soil crusts), our finding is broadly consistent with similar herbarium analyses from Central Great Plains grasslands which also document the onset of foliar N and $\delta^{15}\text{N}$ declines in the 1930s (McLauchlan et al., 2010). Indeed, our study region was among the most strongly affected by the Dust Bowl and was severe in effect across both the NGP and NRM (Fye et al., 2003), consistent with our finding that N declines were independent of ecoregion among common plant species. Regardless of what initially triggered declines in N and $\delta^{15}\text{N}$, however, the fact that they have not recovered to pre-1930's levels, but rather have continued to decline, is consistent with diminished foliar N in the face of sustained eCO₂.

While declines in foliar $\delta^{15}\text{N}$ are consistent with diminished soil N availability, we lack information on how any increases in biomass production and leaf mass area (LMA; g m⁻²) may have influenced declines in foliar N concentrations. FACE experiments document increased LMA in response to eCO₂ (Poorter et al., 2009) and higher declines in N concentrations when expressed per unit leaf mass rather than area (Temme et al., 2017). However, syntheses of FACE results also indicate that declines in foliar N are not explained by dilution from enhanced biomass growth but rather declines in N acquisition and assimilation (Feng et al., 2015), consistent with widespread declines in foliar $\delta^{15}\text{N}$ in response to CO₂ enrichment (BassiriRad et al., 2003). Nevertheless, we do observe relatively large increases in C concentrations among grasses, which could dilute N assuming constant LMA. A large body of evidence indicates that increases in foliar C under eCO₂ result largely from an increase in non-structural carbohydrates (Leakey et al., 2009; Peñuelas & Estiarte, 1996).

Though it remains unclear what specific mechanisms contributed to increased foliar C in our study, we note that grasses can accumulate high levels of silicon (Si) in their leaves, particularly in drier grasslands similar to ours, and trade off Si for C as foliar C increases, especially in low N soils (Quigley et al., 2020). Further, grass Si concentrations have been shown to decline while phenolic compounds increase in response to eCO₂ (Johnson & Hartley, 2018), suggesting that our documented increases in foliar C may have also been accompanied by changes in Si versus C-based structural support and herbivore defense.

Increasing foliar C and decreasing foliar N suggest that C:N ratios will continue to rise (Fig. 4b), a trend that could further constrain plant N supply through greater microbial N immobilization in soils (Feng et al., 2015; Luo et al., 2004). In addition, increases in foliar C:N are associated with decreased leaf protein content and indicate diminished plant nutritional quality for herbivores (Craine et al., 2017; Leakey et al., 2009; Loladze, 2002). Given our evidence for spatially-uniform declines in plant N yet climate-dependency of greening trends, it is possible that projected increases in precipitation and temperature (Stoy et al., 2018) will induce further N deficits and poorer quality forage across the NGP.

In addition to the implications of our results for NGP productivity and herbivore responses, our results have direct implications for how Earth system and vegetation models are parameterized. First, our results confirm constant C_i/C_a and increases in iWUE over the last century, a result that is critical to accurate representation of physiological responses to eCO₂. Yet, the implications of increased iWUE for soil water availability and feedbacks to the N cycle (e.g., mineralization and losses) remain highly uncertain. Second, documented declines in foliar N and $\delta^{15}\text{N}$ have not been integrated into current land models (Thomas et al., 2015) but could provide an important constraint to representation of N limitation in simulations of vegetation response to eCO₂ and climate change. Indeed, vegetative greening in the face of declining foliar N and N/C_i suggests a sustained increase in NUE over the last two decades or more, but it is unclear whether such apparent NUE enhancement will persist in the future.

Our results signal a looming threshold in the ability of N to sustain observed greening trends in NGP grasslands, and support the mounting evidence for declines in plant N availability with eCO₂ across N-limited land areas (Craine et al., 2018; McLauchlan et al., 2017). Future plant and

subsequent ecosystem responses will depend on the extent that physiological adjustments, allocation patterns and shifts in N-acquisition strategies (Terrer et al., 2018) may be sufficient to overcome N limitation. Overall, our findings emphasize the importance of understanding historical changes in biogeochemical functioning for next-generation projections of vegetation responses to eCO₂ and climate.

Acknowledgements

We are grateful to M. Lavin for assistance with herbarium samples at MSU and to N. Davis and B. Leach for assistance in the field and laboratory. We thank J. Craine and an anonymous reviewer for their helpful suggestions on the manuscript. This work was supported by the Montana State University College of Agriculture, the U.S. National Science Foundation awards OIA-1632810, DEB-1552976, and EF-1702029, and the USDA Hatch project 228396.

Author contributions

ENJB designed the study and led data analysis and writing of the paper with help from PCS, BC and BF. BF performed IRMS analyses.

Additional information

Supplementary information is available in the xxxx. Reprints and permissions information is available online at xxx. Correspondence and requests for materials should be addressed to ENJB.

Data availability

The data that support the findings of this study are available from the corresponding author upon reasonable request.

Competing financial interests

The authors declare no competing financial interests.

References

- Anderson, D. R. (2007). *Model based inference in the life sciences: a primer on evidence*. Springer Science & Business Media.
- Auch, R. F., Sayler, K. L., Napton, D. E., Taylor, J. L., & Brooks, M. S. (2011). Ecoregional differences in late-20th-century land-use and land-cover change in the US northern great plains. *Great Plains Research*, 231–243.
- BassiriRad, H., Constable, J. V. H., Lussenhop, J., Kimball, B. A., Norby, R. J., Oechel, W. C., Reich, P. B., Schlesinger, W. H., Zitzer, S., Sehtiya, H. L., & Silim, S. (2003). Widespread foliage $\delta^{15}\text{N}$ depletion under elevated CO_2 : inferences for the nitrogen cycle. *Global Change Biology*, 9(11), 1582–1590. <https://doi.org/10.1046/j.1365-2486.2003.00679.x>
- Bromley, G. T., Gerken, T., Prein, A. F., & Stoy, P. C. (2019). Recent trends in the near-surface climatology of the northern North American Great Plains. *Journal of Climate*. <https://doi.org/10.1175/JCLI-D-19-0106.1>
- Brookshire, E. N. J., & Weaver, T. (2015). Long-term decline in grassland productivity driven by increasing dryness. *Nature Communications*, 6. <http://www.nature.com/ncomms/2015/150514/ncomms8148/full/ncomms8148.html>
- Burke, I. C., Lauenroth, W. K., & Parton, W. J. (1997). Regional and temporal variation in net primary production and nitrogen mineralization in grasslands. *Ecology*, 78(5), 1330–1340.
- Busch, F. A., Sage, R. F., & Farquhar, G. D. (2017). Plants increase CO_2 uptake by assimilating nitrogen via the photorespiratory pathway. *Nature Plants*, 1. <https://doi.org/10.1038/s41477-017-0065-x>
- Craine, J. M., Brookshire, E. N. J., Cramer, M. D., Hasselquist, N. J., Koba, K., Marin-Spiotta, E., & Wang, L. (2015). Ecological interpretations of nitrogen isotope ratios of terrestrial plants and soils. *Plant and Soil*, 1–26.
- Craine, J. M., Elmore, A., & Angerer, J. P. (2017). Long-term declines in dietary nutritional quality for North American cattle. *Environmental Research Letters*, 12(4), 044019. <https://doi.org/10.1088/1748-9326/aa67a4>
- Craine, J. M., Elmore, A. J., Aidar, M. P., Bustamante, M., Dawson, T. E., Hobbie, E. A., Kahmen, A., Mack, M. C., McLauchlan, K. K., & Michelsen, A. (2009). Global patterns of foliar nitrogen isotopes and

their relationships with climate, mycorrhizal fungi, foliar nutrient concentrations, and nitrogen availability. *New Phytologist*, 183(4), 980–992.

Craine, J. M., Elmore, A. J., Wang, L., Aranibar, J., Bauters, M., Boeckx, P., Crowley, B. E., Dawes, M. A., Delzon, S., & Fajardo, A. (2018). Isotopic evidence for oligotrophication of terrestrial ecosystems. *Nature Ecology & Evolution*, 2(11), 1735.

Emmett, K. D., Renwick, K. M., & Poulter, B. (2018). Disentangling Climate and Disturbance Effects on Regional Vegetation Greening Trends. *Ecosystems*. <https://doi.org/10.1007/s10021-018-0309-2>

Farquhar, G. D., Ehleringer, J. R., & Hubick, K. T. (1989). Carbon Isotope Discrimination and Photosynthesis. *Annual Review of Plant Physiology and Plant Molecular Biology*, 40(1), 503–537.

<https://doi.org/10.1146/annurev.pp.40.060189.002443>

Farquhar, G. v, von Caemmerer, S. von, & Berry, J. A. (1980). A biochemical model of photosynthetic CO₂ assimilation in leaves of C₃ species. *Planta*, 149(1), 78–90.

Feng, Z., Rütting, T., Pleijel, H., Wallin, G., Reich, P. B., Kammann, C. I., Newton, P. C. D., Kobayashi, K., Luo, Y., & Uddling, J. (2015). Constraints to nitrogen acquisition of terrestrial plants under elevated CO₂. *Global Change Biology*, 21(8), 3152–3168. <https://doi.org/10.1111/gcb.12938>

Francey, R. J., Allison, C. E., Etheridge, D. M., Trudinger, C. M., Enting, I. G., Leuenberger, M., Langenfelds, R. L., Michel, E., & Steele, L. P. (1999). A 1000-year high precision record of $\delta^{13}\text{C}$ in atmospheric CO₂. *Tellus B*, 51(2), 170–193. <https://doi.org/10.1034/j.1600-0889.1999.t01-1-00005.x>

Frank, D. C., Poulter, B., Saurer, M., Esper, J., Huntingford, C., Helle, G., Treydte, K., Zimmermann, N. E., Schleser, G. H., Ahlström, A., & others. (2015). Water-use efficiency and transpiration across European forests during the Anthropocene. *Nature Climate Change*, 5(6), 579–583.

Fye, F. K., Stahle, D. W., & Cook, E. R. (2003). Paleoclimatic analogs to twentieth-century moisture regimes across the United States. *Bulletin of the American Meteorological Society*, 84(7), 901–910.

Gerken, T., Bromley, G. T., & Stoy, P. C. (2017). Surface Moistening Trends in the Northern North American Great Plains Increase the Likelihood of Convective Initiation. *Journal of Hydrometeorology*, 19(1), 227–244. <https://doi.org/10.1175/JHM-D-17-0117.1>

Guerrieri, R., Belmecheri, S., Ollinger, S. V., Asbjornsen, H., Jennings, K., Xiao, J., Stocker, B. D., Martin, M., Hollinger, D. Y., Bracho-Garrillo, R., Clark, K., Dore, S., Kolb, T., Munger, J. W., Novick, K., & Richardson, A. D. (2019). Disentangling the role of photosynthesis and stomatal conductance on rising forest water-use efficiency. *Proceedings of the National Academy of Sciences*, 116(34), 16909–16914. <https://doi.org/10.1073/pnas.1905912116>

Houlton, B., & Bai, E. (2009). Imprint of denitrifying bacteria on the global terrestrial biosphere. *Proceedings of The National Academy of Sciences Of The United States*, 106(51), 21713–21716.

<https://doi.org/10.1073/pnas.0912111106>

Huang, K., Xia, J., Wang, Y., Ahlström, A., Chen, J., Cook, R. B., Cui, E., Fang, Y., Fisher, J. B., Huntzinger, D. N., Li, Z., Michalak, A. M., Qiao, Y., Schaefer, K., Schwalm, C., Wang, J., Wei, Y., Xu, X., Yan, L., ... Luo, Y. (2018). Enhanced peak growth of global vegetation and its key mechanisms. *Nature Ecology & Evolution*, 1. <https://doi.org/10.1038/s41559-018-0714-0>

Hufkens, K., Keenan, T. F., Flanagan, L. B., Scott, R. L., Bernacchi, C. J., Joo, E., Brunsell, N. A., Verfaillie, J., & Richardson, A. D. (2016). Productivity of North American grasslands is increased under future climate scenarios despite rising aridity. *Nature Climate Change*, 6(7), 710.

Hungate, B., Dukes, J., Shaw, M., Luo, Y., & Field, C. (2003). Nitrogen and climate change. *Science*, 302(5650), 1512–1513.

Johnson, S. N., & Hartley, S. E. (2018). Elevated carbon dioxide and warming impact silicon and phenolic-based defences differently in native and exotic grasses. *Global Change Biology*, 24(9), 3886–3896. <https://doi.org/10.1111/gcb.13971>

Karger, D. N., Conrad, O., Böhner, J., Kawohl, T., Kreft, H., Soria-Auza, R. W., Zimmermann, N. E., Linder, H. P., & Kessler, M. (2017). Climatologies at high resolution for the earth's land surface areas. *Scientific Data*, 4, 170122.

Keeling, C. D., Chin, J. F. S., & Whorf, T. P. (1996). Increased activity of northern vegetation inferred from atmospheric CO₂ measurements. *Nature*, 382(6587), 146.

Lavin, M., & Seibert, C. (2011). Great plains flora? Plant geography of eastern Montana's lower elevation shrub-grass dominated vegetation. *Natural Resources and Environmental Issues*, 16(1), 2.

Leakey, A. D. B., Ainsworth, E. A., Bernacchi, C. J., Rogers, A., Long, S. P., & Ort, D. R. (2009). Elevated CO₂ effects on plant carbon, nitrogen, and water relations: six important lessons from FACE. *Journal of Experimental Botany*, 60(10), 2859–2876. <https://doi.org/10.1093/jxb/erp096>

Loladze, I. (2002). Rising atmospheric CO₂ and human nutrition: toward globally imbalanced plant stoichiometry? *Trends in Ecology & Evolution*, 17(10), 457–461.

Luo, Y., Su, B., Currie, W., Dukes, J., Finzi, A., Hartwig, U., Hungate, B., McMurtrie, R., Oren, R., Parton, W., Pataki, D., Shaw, M., Zak, D., & Field, C. (2004). Progressive nitrogen limitation of ecosystem responses to rising atmospheric carbon dioxide. *BIOSCIENCE*, 54(8), 731–739.

- Mao, J., Ribes, A., Yan, B., Shi, X., Thornton, P. E., Séférian, R., Ciais, P., Myneni, R. B., Douville, H., & Piao, S. (2016). Human-induced greening of the northern extratropical land surface. *Nature Climate Change*, 6(10), 959.
- McLauchlan, K. K., Gerhart, L. M., Battles, J. J., Craine, J. M., Elmore, A. J., Higuera, P. E., Mack, M. C., McNeil, B. E., Nelson, D. M., Pederson, N., & Perakis, S. S. (2017). Centennial-scale reductions in nitrogen availability in temperate forests of the United States. *Scientific Reports*, 7(1), 7856. <https://doi.org/10.1038/s41598-017-08170-z>
- McLauchlan, Kendra K., Ferguson, C. J., Wilson, I. E., Ocheltree, T. W., & Craine, J. M. (2010). Thirteen decades of foliar isotopes indicate declining nitrogen availability in central North American grasslands. *New Phytologist*, 187(4), 1135–1145.
- McMurtrie, R. E., Norby, R. J., Medlyn, B. E., Dewar, R. C., Pepper, D. A., Reich, P. B., & Barton, C. V. (2008). Why is plant-growth response to elevated CO₂ amplified when water is limiting, but reduced when nitrogen is limiting? A growth-optimisation hypothesis. *Functional Plant Biology*, 35(6), 521–534.
- Medlyn, B. E., Duursma, R. A., Eamus, D., Ellsworth, D. S., Prentice, I. C., Barton, C. V., Crous, K. Y., De Angelis, P., Freeman, M., & Wingate, L. (2011). Reconciling the optimal and empirical approaches to modelling stomatal conductance. *Global Change Biology*, 17(6), 2134–2144.
- Mueggler, W. F., Stewart, W. L., & others. (1980). Grassland and shrubland habitat types of western Montana. *US Forest Service, Intermountain Forest and Range Experiment Station, General Technical Report, INT-66*. <http://www.cabdirect.org/abstracts/19802604329.html>
- Myneni, R. B., Keeling, C. D., Tucker, C. J., Asrar, G., & Nemani, R. R. (1997). Increased plant growth in the northern high latitudes from 1981 to 1991. *Nature*, 386(6626), 698.
- Peñuelas, J., & Estiarte, M. (1996). Trends in plant carbon concentration and plant demand for N throughout this century. *Oecologia*, 109(1), 69–73.
- Peñuelas, J., & Matamala, R. (1990). Changes in N and S leaf content, stomatal density and specific leaf area of 14 plant species during the last three centuries of CO₂ increase. *Journal of Experimental Botany*, 41(9), 1119–1124.
- Poorter, H., Niinemets, Ü., Poorter, L., Wright, I. J., & Villar, R. (2009). Causes and consequences of variation in leaf mass per area (LMA): a meta-analysis. *New Phytologist*, 182(3), 565–588.
- Quigley, K. M., Griffith, D. M., Donati, G. L., & Anderson, T. M. (n.d.). Soil nutrients and precipitation are major drivers of global patterns of grass leaf silicification. *Ecology*, n/a(n/a), e03006. <https://doi.org/10.1002/ecy.3006>

- Reeves, M. C., Moreno, A. L., Bagne, K. E., & Running, S. W. (2014). Estimating climate change effects on net primary production of rangelands in the United States. *Climatic Change*, *126*(3–4), 429–442.
- Reich, P. B., & Hobbie, S. E. (2013). Decade-long soil nitrogen constraint on the CO₂ fertilization of plant biomass. *Nature Climate Change*, *3*(3), 278.
- Rodell, M., Famiglietti, J. S., Wiese, D. N., Reager, J. T., Beaudoin, H. K., Landerer, F. W., & Lo, M.-H. (2018). Emerging trends in global freshwater availability. *Nature*, *557*(7707), 651.
- Shafer, S. L., Bartlein, P. J., Gray, E. M., & Pellier, R. T. (2015). Projected Future Vegetation Changes for the Northwest United States and Southwest Canada at a Fine Spatial Resolution Using a Dynamic Global Vegetation Model. *PloS One*, *10*(10), e0138759.
- Still, C. J., Berry, J. A., Collatz, G. J., & DeFries, R. S. (2003). Global distribution of C₃ and C₄ vegetation: Carbon cycle implications. *Global Biogeochemical Cycles*, *17*(1), 6-1-6–14.
<https://doi.org/10.1029/2001GB001807>
- Stoy, P. C., Ahmed, S., Jarchow, M., Rashford, B., Swanson, D., Albeke, S., Bromley, G., Brookshire, E. N. J., Dixon, M. D., Haggerty, J., Miller, P., Peyton, B., Royem, A., Spangler, L., Straub, C., & Poulter, B. (2018). Opportunities and Trade-offs among BECCS and the Food, Water, Energy, Biodiversity, and Social Systems Nexus at Regional Scales. *BioScience*, *68*(2), 100–111.
<https://doi.org/10.1093/biosci/bix145>
- Temme, A. A., Liu, J. C., van Hal, J., Cornwell, W. K., Cornelissen, J. H. H., & Aerts, R. (2017). Increases in CO₂ from past low to future high levels result in “slower” strategies on the leaf economic spectrum. *Perspectives in Plant Ecology, Evolution and Systematics*, *29*, 41–50.
- Terrer, C., Vicca, S., Stocker, B. D., Hungate, B. A., Phillips, R. P., Reich, P. B., Finzi, A. C., & Prentice, I. C. (2018). Ecosystem responses to elevated CO₂ governed by plant–soil interactions and the cost of nitrogen acquisition. *New Phytologist*, *217*(2), 507–522.
- Thomas, R. Q., Brookshire, E. N. J., & Gerber, S. (2015). Nitrogen limitation on land: how can it occur in Earth system models? *Global Change Biology*, *21*(5), 1777–1793. <https://doi.org/10.1111/gcb.12813>
- Zhu, Z., Piao, S., Myneni, R. B., Huang, M., Zeng, Z., Canadell, J. G., Ciais, P., Sitch, S., Friedlingstein, P., Arneeth, A., Cao, C., Cheng, L., Kato, E., Koven, C., Li, Y., Lian, X., Liu, Y., Liu, R., Mao, J., ... Zeng, N. (2016). Greening of the Earth and its drivers. *Nature Climate Change*, *6*(8), 791–795.
<https://doi.org/10.1038/nclimate3004>

Table 1 Geometric mean and geometric standard deviation range (in parentheses) of greening (increasing NDVI) and browning (decreasing NDVI) across the northern Great Plains (NGP), the Montana (MT) portions of the NGP (MT_{NGP}) and the Montana portions of the northern Rocky Mountains (MT_{NRM}).

	NGP	MT _{NGP}	MT _{NRM}
Land area greening (%)	19.4	19.1	15.2
Land area browning (%)	2.2	1.2	7.6
Greening pixel rate (% yr ⁻¹)	1.21 (0.44 – 3.31)	1.53 (0.63 – 3.68)	0.56 (0.19 – 1.63)
Browning pixel rate (% yr ⁻¹)	-0.34 (-0.09 – -1.15)	-0.53 (-0.15 – -1.91)	-0.37 (-0.13 – -1.09)
Net greening rate (% yr ⁻¹)	0.23 (0.09 – 0.71)	0.28 (0.13 – 0.75)	0.06 (0.04 – 0.37)

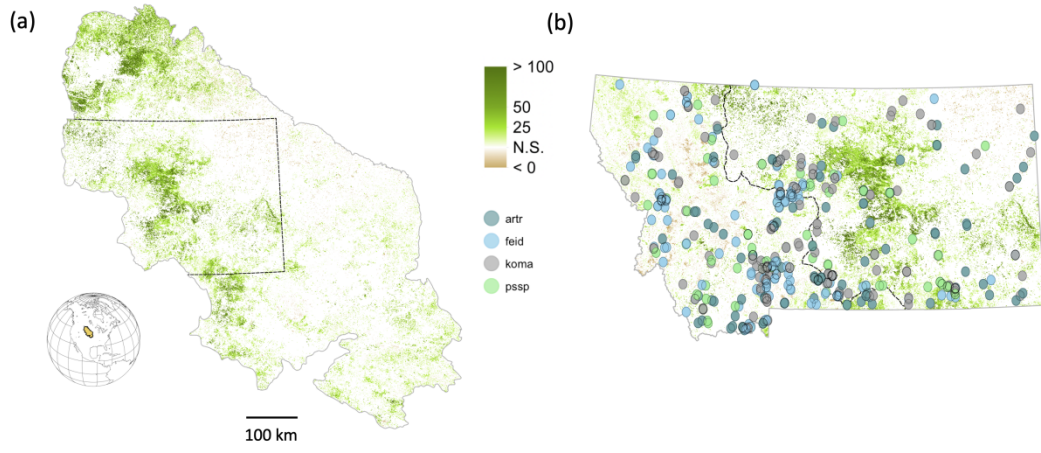
Figure Legends

FIGURE 1 Recent patterns of vegetation greening across the Northern Great Plains (NGP) of North America. Percent change in NDVI from 2000 to 2018 across the NGP (a). White areas show pixels with no evidence of significant change. The inset in (a) shows study area location within the NGP (tan color). Distribution of herbarium samples across the NGP and Northern Rocky Mountains (NRM) of MT (b). Species are *Artemisia tridentata* (artr), *Festuca idahoensis* (feid), *Koeleria macrantha* (koma) and *Pseudoregeneria spicata* (pssp). The dashed line indicates the boundary between the NGP (east) and NRM (west) ecoregions.

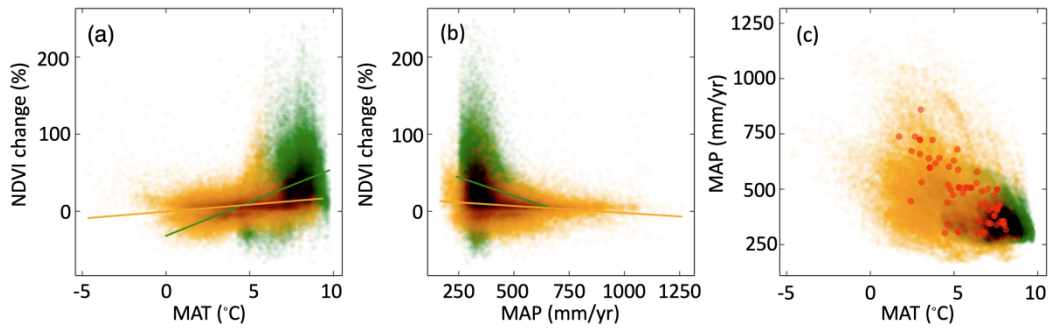
FIGURE 2 Distribution of vegetative greening rates across our study area. Shown is NDVI change over the 2000-2018 period in the NGP (green points and regression lines) and NRM (orange points and regression lines) as a function of mean annual temperature (a) and precipitation (b). Panel (c) shows the distribution of 2016 herbarium sampling locations across climate space of the NGP and NRM.

FIGURE 3 Regional climate patterns and vegetation chemical change. Time series of growing season Palmer Drought Severity Index (PDSI; lower values indicate drought conditions) for hydrologic basins in the NGP (green lines) and NRM (orange lines; a). Z-scores of atmospheric N deposition (b), leaf internal CO₂ (C_i) concentrations (c), foliar N (d), water use efficiency (e), and foliar $\delta^{15}\text{N}$ (f). Vertical dashed lines show significant ($p < 0.05$) breakpoints in slope determined using segmented regression for N and $\delta^{15}\text{N}$ (green) and C_i (black). AICc was lowest in linear mixed effects models with species identity only as a random effect. Species colors in (c-f) are the same as in Fig. 1.

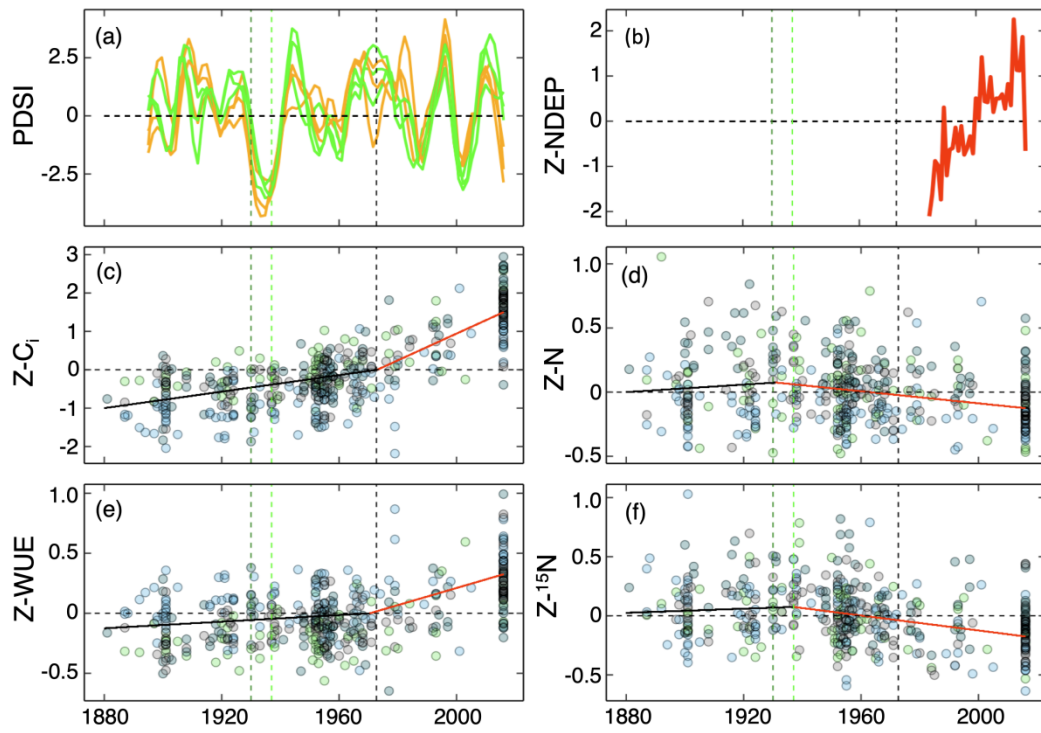
FIGURE 4 Functional response of foliar chemistry and $\delta^{15}\text{N}$ to increasing leaf internal CO₂ concentration (C_i). Species-specific saturating curves across the full historical data set for foliar %C (a), %N (b), foliar C:N ratios (c) $\delta^{15}\text{N}$ (d). Thin lines with arrows connect historic and contemporary samples and thick lines are fitted curves through all samples. Vertical dashed lines show the break-point year value of C_i .



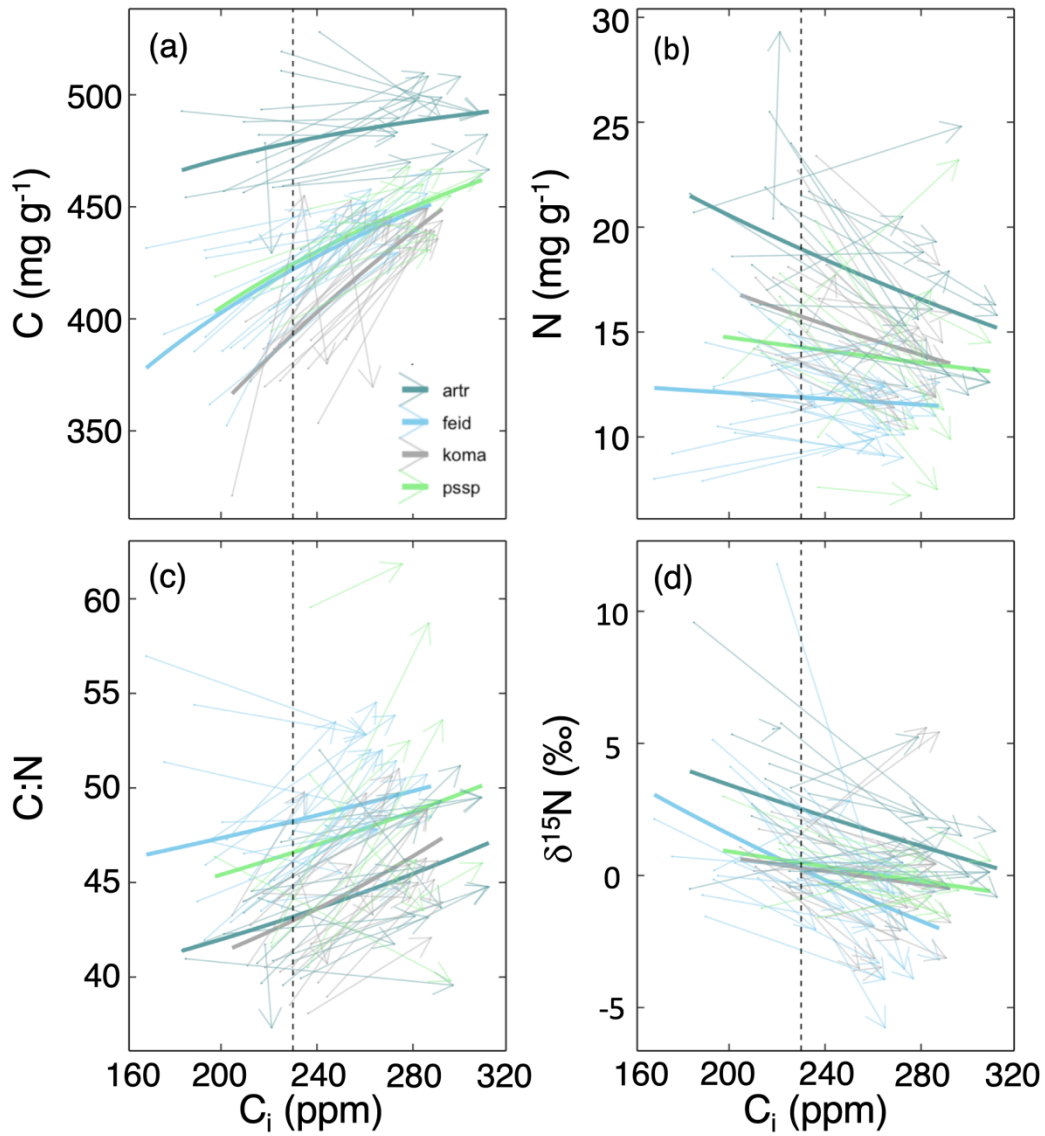
gcb_15115_f1.png



gcb_15115_f2.png



gcb_15115_f3.png



gcb_15115_f4.png